PCCP

Magnetic Susceptibility of Actinide(III) Cations: Experimental and Theoretical Study.

Journal:	*Physical Chemistry Chemical Physics*
Manuscript ID	CP-ART-12-2015-007456.R1
Article Type:	Paper
Date Submitted by the Author:	19-Jan-2016
Complete List of Authors:	Autillo, Matthieu; CEA, RadioChemistry & Processes Department Berthon, Claude; CEA/DEN/DRCP, Guerin, Laetitia; CEA/DEN/DRCP Bolvin, Helene; Universite Toulouse, Laboratoire de Chimie Physique Quantique Moisy, Philippe; CEA,

SCHOLARONE™
Manuscripts

Journal Name

RSCPublishing

ARTICLE

Magnetic Susceptibility of Actinide(III) Cations: Experimental and Theoretical Study

Cite this: DOI: 10.1039/xoxxoooooox

Received ooth January 2012,
Accepted ooth January 2012

DOI: 10.1039/xoxxoooooox

www.rsc.org/

Matthieu Autillo[a], Laetitia Guerin[a], Hélène Bolvin[b], Philippe Moisy[a] and Claude Berthon*[,a].

[a] CEA, Nuclear Energy Division, RadioChemistry & Processes Department, DRCP, BP 17171, F-30207 Bagnols sur Cèze, France. Fax: +33 4 66 79 63 25; Tel: +33 4 66 79 65 69; E-mail: claude.berthon@cea.fr.

[b] Laboratoire de Physique et de Chimie Quantiques, Université Toulouse 3, 118 Route de Narbonne, 31062 Toulouse, France.

In a previous paper, the influence of radioactive decay (α and β^-) on magnetic susceptibility measurements by the Evans's method has been demonstrated by the study of two americium isotopes. To characterize more accurately this phenomenon and particularly their influence on the Curie law, a new study has been performed on two uranium isotopes (^{238}U and ^{233}U) and on tritiated water (^3H_2O). The results on the influence of α emissions have established a relationship between changes in the temperature dependence and the radioactivity in solution. Regarding the β^- emissions, less influence was observed while no temperature dependence linked to this kind of radioactive emission could be identified. Once magnetic susceptibility measurements of actinide (III) cations were corrected from radioactivity effects, methods of quantum chemistry have been used on free ions and aquo complexes to calculate the electronic structure explaining magnetic properties of Pu(III), Am(III) and Cm(III). The ligand field effect on the magnetic behavior (Curie constant and temperature-independent susceptibilities) was analyzed by considering different solvation environments.

1. Introduction

Recently, magnetic susceptibility measurements performed by NMR spectroscopy on actinide ions in solutions revealed deviations from the Curie law based on the Hund's rules of free ions[1]. The Evans' NMR method[2], used to make these Bulk Magnetic Susceptibility (BMS) measurements in perchloric medium, showed a paramagnetic behavior of these An(III) cations in contradiction with other measurements previously performed on solids aquo complexes[3]. Given their low paramagnetic behavior, requiring higher concentrations in solution unlike most of the other actinide ions, it was suggested that the radioactivity of these elements can lead to an overvaluation of their magnetic susceptibilities measured by this method. A previous study[4] confirmed this hypothesis by considering the influence of different radioactive decay (α and β^-) through measurements performed on two americium samples (^{241}Am and ^{243}Am). These isotopes have distinct radioactive α decay ($T_{1/2}$ = 433 days and $T_{1/2}$ = 7380 days respectively) but also, the ^{243}Am decay produces ^{239}Np which is β^- with a short period ($T_{1/2}$ = 2.4 days). This chemical system allowed to show that the formation of short life paramagnetic radicals (e^-_{aq}, °H, °OH...), continuously generated in solution by α water radiolysis[5, 6], leads to a linear increase of the magnetic susceptibility for high dose rates. The study of these samples at different temperatures showed a shift of both the magnetic susceptibility at 25°C and the Curie constant depending on the radioactivity of the solution. However, this work was not able to clearly characterize this phenomenon in particular for low α radioactivity. On the other hand, the study of the ^{239}Np production by ^{243}Am decay showed a correlation between the β^- radioactivity and the increase of the magnetic susceptibility. This increase in magnetic susceptibility due to β^- emission was found 23 times larger than that due to α particles for the same radioactivity. However, the influence of β^- particles emissions in solution cannot be separated from the formation of secondary products generated by the recombination of radicals over time and the magnetic susceptibility increase could not be clearly identified.

The main objective of this study is to characterize accurately the paramagnetic behavior of An(III) cations in aqueous solution regardless of their radioactive nature. Therefore, it is necessary to further describe the effect of α and β^- emissions but also to isolate their influence on the Curie law. To separate the effects of α and β^- emissions, two studies were conducted. For the influence of the α radioactivity, ^{238}U/^{233}U isotopes were chosen because of their significant difference in radioactive decay ($T_{1/2} = 4.5 \cdot 10^9$ years and $T_{1/2} = 159 \cdot 10^3$ years respectively). Furthermore, uranium in oxidation state +VI is closed shell and shows Temperature-

Independent Paramagnetism (TIP). This feature is particularly interesting in order to quantify the slightest temperature dependence due to the radicals generated by α radiolysis. To observe the influence of the β^- particles, tritiated water was used. This isotope (^3H) is a pure β^- transmitter with an average energy of 5.6 keV and a short radioactive decay ($T_{1/2}$ = 12.3 years). Its use in different proportions in the aqueous phases of Nd(III) will clearly identify the effect of this kind of radioactive decay on magnetic susceptibility measurements independently of any other radioactivity. The Nd(III) cation was selected for its paramagnetic properties providing a correct ^1H chemical shift for a concentration range directly measurable by UV-visible-near IR spectrophotometry (UV-vis-NIR).

Finally, in order to rationalize the experimental magnetic susceptibilities, quantum chemistry calculations were performed. The calculation of magnetic properties of actinide compounds are challenging due to the importance of both relativistic and correlation effects. Since the calculation of magnetic properties of U(III) complexes with the wave-function based method SO-CASPT2 gives good agreement with experimental data[7,8], the same method was used in the present work. The combination of experimental data and theoretical calculations permits a better understanding of magnetic properties of the 5f elements.

2. Experimental and computational details

^1H NMR spectra were recorded using 400 MHz Fourier transform spectrometers, Agilent DD2, set up for the study of radioactive samples. BMS were collected at every 5K step in several temperature ranges. After each experiment, a new measurement at 298K was performed to check the sample stability.

UV-vis-NIR spectra were recorded with a Cary 50 spectrophotometer using a 1cm optical path quartz cell.

Determinations of actinide concentrations with α and γ spectrometry were performed using a Canberra spectrometer (electronic resolution: 120 keV) with a PIPS detector and a Canberra spectrometer (electronic resolution: 100 keV – 2000 keV) with a germanium N-type detector respectively.

Determinations of uranium concentrations by X-ray fluorescence spectrometry were performed using a Metorex spectrometer equipped with an ^{241}Am source of initial activity 1110 MBq (9/1994).

2.1. Sample preparations

All actinide stocks were drawn from existing solutions or solids prepared at CEA Marcoule. The solution acidities were adjusted using stock solutions of perchloric acid prepared from concentrated perchloric acid. For all the cations examined, oxidation states were checked by UV-vis-NIR just prior to and immediately after each NMR experiments (**Figure ESI 1** – **Figure ESI 5** of SI).

Americium:

For magnetic susceptibility measurements, the isotopic composition of the americium solution was 98.739% 241, 0.01% 242 and 1.251% 243. The same samples to those described in our previous work[4] were used to perform these measurements at different temperature (**sample 1-1 to 1-4**).

Plutonium:

For magnetic susceptibility measurements, the isotopic composition of the plutonium solution was 0.082% 238, 81.498% 239, 17.296% 240, 0.747% 241 and 0.377% 242. The Pu(III) (**sample 2**) was prepared by dissolving hydrated $Pu(OH)_4$ (s) precipitate in a volume of perchloric acid containing an appropriate quantity of hydroxylammonium perchlorate. The conversion of plutonium from Pu(IV) to Pu(III) was observed by spectrophotometry monitoring and the concentration of this solution was measured by these absorption spectra ($C_{Pu(III)}$ = 0.157 (±0.004) mol.L^{-1}).

Uranium:

The U(VI) solution (**sample 3**) was prepared by dissolving solid UO_3 (natural uranium: 99.29% 238 and 0.71% 235) in perchloric acid. The determination of uranium concentration was performed by X-ray fluorescence and UV-vis-NIR spectrophotometry ($C_{U(VI)}$ = 0.57 (±0.01) mol.L^{-1}).

For magnetic susceptibility measurements at different α radioactivity, the isotopic composition of the uranium solution was 90.550% 233, 0.521% 234, 0.109% 235 and 8.820% 238. The U(VI) solution (**sample 4-1**) was prepared by dissolving hydrated $UO_2(OH)_2$ (s) precipitate in an appropriate volume of perchloric acid. Uranium concentration adjustments (**samples 4-2 to 4-4**) were performed by successive dilutions of the stock solution which was the starting point of susceptibility measurements.

Curium:

For magnetic susceptibility measurements, the isotopic composition of the curium solution was 0.90% 243, 72.17% 244, 12.68% 245, 13.09% 246, 0.59% 247, 0.57% 248. The Cm(III) (**sample 5**) was prepared by dissolving hydrated $Cm(OH)_3$ (s) precipitate in a minimum volume of perchloric acid. The determination of curium concentration of this solution was performed by α counting ($C_{Cm(III)}$ = 1.62 (±0.04)·10^{-3} mol.L^{-1}).

Table 1: Actinide samples compositions.

Sample		$[An^{n+}]$ (mol.L^{-1})	$[HClO_4]$ (mol.L^{-1})	$[ClO_4^-]_{tot}$ (mol.L^{-1})	[t-BuOH] (mol.L^{-1})
Am(III)	1-1	[a] 0.096 (±0.003)	1	1.3	0.2
	1-2	[a] 0.036 (±0.001)	1	1.1	0.3
	1-3	[a] 0.024 (±0.001)	1	1.1	0.3
	1-4	[a] 0.122 (±0.006)	1	1.3	0.2
Pu(III)	2	[b] 0.157 (±0.004)	1	3.1	0.2
U(VI)	3	[c] 0.57 (±0.01)	1	2.1	0.2
	4-1	[d] 1.23 (±0.06)	1	4	0.2
	4-2	[d] 0.90 (±0.05)	1	3.2	0.15
	4-3	[d] 0.82 (±0.04)	1	3	0.13
	4-4	[d] 0.55 (±0.03)	1	2.3	0.09
Cm(III)	5	[e] 1.62 (±0.04)·10^{-3}	1	1	0.2

[a] *average concentration determined by γ counting et spectrophotometry (ε_{503nm} = 368 L.cm^{-1}.mol^{-1})[9].*

[b] *concentration determined by spectrophotometry (ε_{560nm} = 37 L.cm^{-1}.mol^{-1})[10].*

[c] *average concentration determined by X-ray fluorescence spectrometry and spectrophotometry (ε_{416nm} = 7.8 L.cm^{-1}.mol^{-1}).*

[d] *concentration determined by spectrophotometry (ε_{416nm} = 7.8 L.cm^{-1}.mol^{-1}).*

[e] *concentration determined by α counting.*

Neodymium:

The Nd(III) stock solution was prepared by dissolving natural solid $NdCl_3$-xH_2O (99.9%, Sigma-Aldrich) in 1M perchloric acid. The stock solution of tritiated water contains a β^- initial activity of 3.4·10^{11} Bq.L^{-1}. Our acquisition being fast compared to the ^3H radioactive decay, the radioactivity variation over time was not taken

This journal is © The Royal Society of Chemistry 2012

Table 2: Nd(III) samples compositions.

Sample	6-1	6-2	6-3	6-4	6-5	6-6	6-7	6-8	6-9
$[Nd^{3+}]$ (mol.L^{-1})	$6.25\cdot10^{-2}$	$6.29\cdot10^{-2}$	$6.17\cdot10^{-2}$	$6.23\cdot10^{-2}$	$6.25\cdot10^{-2}$	$6.19\cdot10^{-2}$	$6.19\cdot10^{-2}$	$6.30\cdot10^{-2}$	$6.27\cdot10^{-2}$
β^- radioactivity (GBq.L^{-1})	323	272	170	136	113	85.0	68.0	56.7	0

$[HClO_4]$ = 1M; [t-BuOH] = 0,2M.

into account. Samples with different β^- radioactivity were prepared by dilution of the Nd(III) stock solution in deuterated and tritiated perchloric acid solution (**samples 6-1 to 6-9**, see Table 2).

2.2. Measurements

The molar magnetic susceptibilities $\chi_{M,meas.}$ of samples were calculated by chemical shift difference $\Delta\delta$ between ^{1}H NMR signal of working (t-BuOH in) and reference (t-BuOH out) solution using the Evans method[2].

$$\chi_{M,meas} = \frac{3\Delta\delta}{10^3[An^{n+}]} \qquad (1)$$

where $\Delta\delta$ is dimensionless, $[An^{n+}]$ is the molar concentration (mol.L^{-1}) of the paramagnetic element and $\chi_{M,meas}$ the molar magnetic susceptibility measured (m^3.mol^{-1}).

A systematic correction due to the composition difference between the working and reference solution ($\Delta\chi_{ref}$) was applied to the magnetic susceptibility measured for each sample. The molar magnetic susceptibility (χ_M) can be expressed by the following equation:

$$\chi_M = \Delta\chi_{ref} + \chi_{M,meas} = \Delta\chi_{ref} + \frac{3\Delta\delta}{10^3[An^{n+}]} \qquad (2)$$

Indeed, it has been observed that perchlorate ions (ClO_4^-) were responsible for slight temperature dependence (**Figure ESI 6** of SI). The high concentrated actinide solutions being prepared by dissolving actinide hydroxides, a significant quantity of $HClO_4$ is necessary to get a molar acidity. This sample preparation protocol generates an additional amount of perchlorate anions in the working solution which is necessary to correct.

Uncertain values were estimated by taking into account $\Delta\delta$ accuracies of NMR measurements and concentrations gained from α/γ counting, X-ray fluorescence spectrometry and UV-vis-NIR spectrophotometry.

2.3. Computational details

The aquo complexes $[An(H_2O)_9]^{3+}$ have been described using the first-principle method SO-CASPT2 using the MOLCAS 8.0 suite of programs[11]. The first coordination sphere made up of nine water molecules was considered. Indeed, comparison of the structures of solids compounds $[An(H_2O)_9](CF_3SO_3)_3$ obtained by Apostolidis[3] with the EXAFS spectra of aquo ions in aqueous solution[12-17] confirms a coordination of An^{3+} ions by nine water molecules in solution. Only the first coordination sphere has been considered during the calculations to describe the aquo complexes in solution.

Table 3: Bond length An-OH$_2$ determined by EXAFS in aqueous solution for the An(III) cations[16].

	Ion	Medium	An – O (Å)
An(III)	Pu^{3+}	1M HCl	2.49(1)
	Am^{3+}	0.05M $HClO_4$	2.47(1)
	Cm^{3+}	0.01M HNO_3	2.46(1)

The geometry of the hydrated actinide ions were optimized at the DFT level of theory with Gaussian 09 program package[18], constraining the An-O distance to the EXAFS one (**Table 3**). Additional SO-CASPT2 calculations were further performed by varying the An-O distances in order to determine their influence on computed properties. The geometry optimizations were performed using the B3LYP functional and an implicit solvation model (IEFPCM) as implemented in G09. Actinides small-core relativistic effective core potentials (RECP) were used together with the accompanying basis set, (14s13p10d8f) contracted to [10s9p5d4f][19]. For other atoms, the 6-31+G(d,p) basis set was used. Calculations were performed without any symmetry.

All atoms are described with all electron basis sets ANO-RCC[20, 21], An and O atoms with TZP and DZP, respectively. The active space consists of n electrons in the 7 5*f* orbitals for an atom of configuration $5f^n$. First, a multi-state CASSCF (Complete Active Space Self Consistent Field) calculation is performed[22]. Dynamical correlation is calculated using the MS-CASPT2 method[23].

For Pu, 21 sextets, 80 quartets and 40 doublets are considered. For Am, 7 septets, 40 quintets, 20 triplets and 20 singlets and for Cm, 1 octuplet, 48 sextets, 76 quartets and 40 doublets. Spin-orbit coupling is evaluated as a state interaction between all MS-CASPT2 wave functions by the RASSI (Restricted Active Space State Interaction) method[24]. Spin-Orbit (SO) integrals are evaluated within the AMFI approximation[25]. The calculation of all the properties is implemented in a local program. g factors are calculated according to reference[26] and magnetic susceptibility according to Eq. **(7)**. Calibration calculations have been performed on the free ions at Hartree-Fock level by means of the numerical code GRASP[27].

3. Results and Discussion

3.1. Theoretical approach

The Hamiltonian describing the molecular system in an external magnetic field $\boldsymbol{B}$ is

$$\hat{H} = \hat{H}^{ZFS} + \hat{H}^{ZE} \qquad (3)$$

where $\hat{H}^{ZFS}$ is the Hamiltonian in the absence of any external field and $\hat{H}^{ZE}$ the Zeeman operator which accounts for the interaction between the magnetic field and the electronic angular momenta.

$$\hat{H}^{ZE} = -\widehat{\boldsymbol{M}}\cdot\boldsymbol{B} = \mu_B\left(\hat{\boldsymbol{L}} + g_e\hat{\boldsymbol{S}}\right)\cdot\boldsymbol{B} \qquad (4)$$

where μ_B is the Bohr magneton, g_e the g-factor of the free ion and $\hat{\boldsymbol{L}}$ and $\hat{\boldsymbol{S}}$ are the orbital and spin angular momenta. The eigen-functions of $\hat{H}$ are denoted $|\Psi_I(\boldsymbol{B})>$ with corresponding energies $E_I(\boldsymbol{B})$ and magnetic moments $\boldsymbol{M}_I(\boldsymbol{B}) = \langle\Psi_I(\boldsymbol{B})|\widehat{\boldsymbol{M}}|\Psi_I(\boldsymbol{B})\rangle$. The thermal average

(5)

magnetization in direction $\boldsymbol{u}$ for an external magnetic field $\boldsymbol{B} = B\boldsymbol{u}$ at temperature T is expressed as follows

$$M_{\boldsymbol{u}}(B,T) = \frac{\sum_I \boldsymbol{M}_I(\boldsymbol{B})\, e^{-E_I(\boldsymbol{B})/kT}}{\sum_I e^{-E_I(\boldsymbol{B})/kT}}$$

where k is the Boltzmann constant. The powder averaging is calculated as

$$M(B,T) = \int_{\boldsymbol{u}} M_{\boldsymbol{u}}(B,T)d\boldsymbol{u} \qquad \textbf{(6)}$$

and the magnetic susceptibility is

$$\chi(T) = \frac{1}{B}\, M(B,T) \qquad \textbf{(7)}$$

The energy $E_I(\boldsymbol{B})$ may be expanded through a Taylor series in terms of B

$$E_I(\boldsymbol{B}) = \mathrm{E}_I + E^{(1)}_{I,\boldsymbol{u}}B + E^{(2)}_{I,\boldsymbol{u}}B^2 + \cdots \qquad \textbf{(8)}$$

where E_I is the energy of level I in absence of external magnetic field and $E^{(1)}_{I,\boldsymbol{u}}$ and $E^{(2)}_{I,\boldsymbol{u}}$ are called first- and second-order Zeeman coefficients. In the limit where B/kT is small, Eq. **(5)** leads to the Van Vleck equation

$$\chi_{\boldsymbol{u},M} = \frac{N_A \sum_I \left[\frac{E^{(1)2}_{I,\boldsymbol{u}}}{kT} - 2E^{(2)}_{I,\boldsymbol{u}}\right] e^{-E_I/kT}}{\sum_I e^{-E_I/kT}} \qquad \textbf{(9)}$$

where N_A is the Avogadro constant. In the case where the ground level of the free ion is a J level well separated in energy from the first excited level, the sum in Eq. **(9)** may be restricted to the $2J+1$ manifold and providing that the zero-field splitting of the J level is small, $E_I \ll kT$, this leads, whatever $\boldsymbol{u}$, to the Curie law

$$\chi_M = \frac{N_A\mu_B g_J^2 J(J+1)}{3kT} = \frac{C}{T} \qquad \textbf{(10)}$$

where g_J is the Landé g-factor and $C = N_A\mu_B g_J^2 J(J+1)/3k$ is the Curie constant.

In the case where the ground level corresponds to $J = 0$ and the next level is high enough not to be populated, the energy of the ground level (Eq. **(8)**) may be expanded as

$$E_0(\boldsymbol{B}) = \mathrm{E}_0 + \sum_{I\neq 0} \frac{\left|\langle\Psi_0(0)|\hat{\boldsymbol{M}}|\Psi_I(0)\rangle\right|^2}{E_0 - E_I} B^2 \qquad \textbf{(11)}$$

and Eq. **(9)** leads to

$$\chi = -2N_A E_0^{(2)} = -2N_A \sum_{I\neq 0} \frac{\left|\langle\Psi_0(0)|\hat{\boldsymbol{M}}|\Psi_I(0)\rangle\right|^2}{E_0 - E_I} \qquad \textbf{(12)}$$

The susceptibility is then independent of temperature: this is the Temperature-Independent Paramagnetism (TIP).

In the case where the $2J+1$ ground manifold has a small zero-field splitting and the next J level is thermally non populated but has a non-negligible Zeeman interaction with the ground level, Eq. **(8)** leads to, for $I = 1,2J+1$

$$E_I(\boldsymbol{B}) = \mathrm{E}_I + \mu_B \mathrm{I} g_J + \sum_{K>2J+1} \frac{\left|\langle\Psi_K(0)|\hat{\boldsymbol{M}}|\Psi_I(0)\rangle\right|^2}{E_I - E_K} B^2 \quad \textbf{(13)}$$

The sum of Eq. **(9)** is limited to the $2J+1$ l first states. Supposing that $E_I \ll kT$, one gets

$$\chi_M = \frac{N_A\mu_B g_J^2 J(J+1)}{3kT} - 2N_A \langle \sum_{I=1}^{2J+1} \sum_{K>2J+1} \frac{\left|\langle\Psi_0(0)|\hat{\boldsymbol{M}}|\Psi_I(0)\rangle\right|^2}{E_I - E_K} \rangle$$
$$= \frac{C}{T} + \chi_{TI} \qquad \textbf{(14)}$$

where $\langle\ \ \rangle$ denotes a powder averaging. In this case, the temperature dependent-part of the susceptibility follows the Curie law and the temperature-independent one characterizes the interaction with the states arising from the first excited *J* manifold.

3.2. Radioactivity influence on BMS measurements

α emission influence. In order to characterize the magnetic behavior of the actinide cations without radioactive decay, magnetic susceptibility measurements on ^{241}Am and ^{233}U in various concentrations were carried out on the temperature range 278-323K. Both Am(III) and U(VI) are expected to behave as TIP. However because we surmised a Curie like law tendency of the magnetic susceptibility values, χ_M has been featured versus 1/T in the range 278-323 K for all these samples. A good correlation has been found by using the equation

$$\boldsymbol{\chi_M = \frac{a}{T} + b}$$

where a is the slope and b the y-intercept of the BMS curves versus 1/T. α radioactivity, magnetic susceptibility (χ_M) at 298K and the slope a are summarized **Table 4**. The slope a arising from the temperature variation of χ_M confirms the presence of radicals issued from the α-decay. Considering that all these radicals are spin ½, they behave within the same Curie constant as defined in Eq. **(10)** which can be assigned to the slope a proportional to the radical concentration. The y-intercept b depends essentially on the second-order Zeeman coefficient of the actinide cation since a TIP behavior is expected for Am(III) and U(VI). Indeed, two series of b values are observed **Table 4** for both cations but with significant uncertainties. The experimental temperature range far from the y-intercept account for these ill-defined values. Regarding a values, it can be seen that magnetic susceptibility increases with the α radioactivity in solution. This confirms previous results exhibiting that α radioactivity affects the measurements obtained with the Evans' method[4].

Table 4: α radioactivity, molar magnetic susceptibility at 298K and slope *a* and b as defined in Eq. (15) of the Am(III) and U(VI) samples.

Sample		α radioactivity ($GBq.L^{-1}$)	χ_M (10^{-8} $m^3.mol^{-1}$)	Slope *a* (10^{-8} $m^3.K.mol^{-1}$)	*b* (10^{-8} $m^3.mol^{-1}$)
Am(III)	*1-1	2940	1.41 (±0.04)	220	0.678
	1-2	1090	1.19 (±0.03)	178	0.596
	1-3	722	1.14 (±0.02)	166	0.590
	*1-4	399	1.16 (±0.03)	128	0.724
U(VI)	4-1	93.0	0.168 (±0.003)	74	-0.080
	4-2	68.0	0.138 (±0.003)	42	0.008
	4-3	62.0	0.136 (±0.003)	35	0.018
	4-4	41.6	0.110 (±0.002)	5	0.094
	3	$1.67\cdot10^{-3}$	0.091 (±0.002)	1	0.087

** Results published in ref [4]*

The slope a values as a function of α radioactivity in solution are shown in **Figure 1**, displaying a nonlinear variation. Indeed, there is a rapid increase at low α radioactivity and there is a plateau for larger values. This variation can be explained by a change in the lifetime of the radical species based on α radioactivity. Thus, for a low radioactivity, the radicals formed by water radiolysis are dispersed in solution and must migrate to recombine and to form molecular species[5, 28, 29]. The radicals' lifetime in solution is conditioned by this diffusion step. The amount of radicals produced in solution increases with the

This journal is © The Royal Society of Chemistry 2012

radioactivity of the solution (30 GBq.L^{-1} – 200 GBq.L^{-1}), which causes a fast rise in temperature dependence. For higher radioactivity (A > 200 GBq.L^{-1}), the heterogeneous areas are likely to overlap in solution which promotes the formation of molecular products[28]. The radicals' lifetime decreases because the probability of encountering another radical species generated in solution increases. The diffusion step is becoming shorter and seems to lead to a stabilization of the amount of radicals present in the solution resulting from a balance between production by water radiolysis and recombination in molecular species.

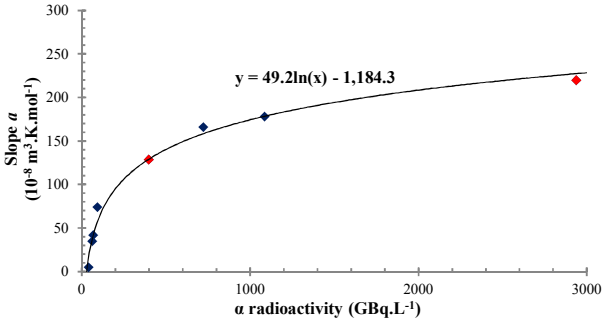

Figure 1: Slope *a* variation vs. α radioactivity for Am(III) and U(VI) samples in 1M perchloric medium (● in this study ; ● in ref [4]).

Considering that the radicals' quantity variation versus α radioactivity can be adjusted by a logarithmic function (see **Figure 1**), a Curie constant related to α radioactivity in solution can be calculated. It may be noted that it becomes negligible for α radioactivity of less than 30 GBq.L^{-1}. Thus, for any radioactivity above this value, the magnetic behavior of the radioactive cation can be corrected by the contribution from the radicals through following equations:

$$\chi_{M,corrected-\alpha} = \chi_M - \chi_{M,\alpha} \qquad \textbf{(16)}$$

$$\chi_{M,\alpha} = \frac{a}{T} = \frac{49.2 \times ln(\alpha\ radioactivity) - 1184.3}{T}$$

with the α radioactivity in Bq.L^{-1} and the temperature T in Kelvin.

β$^-$ emission influence. In our previous study[4], it was shown that β$^-$ emissions had an influence on the magnetic susceptibility measurements performed by the Evans' method. Indeed, a linear increase of the magnetic susceptibility as a function of the β$^-$ radioactivity (^{239}Np) in solution was observed. This study could be considered imprecise because conducted simultaneously in the presence of degradation products formed by α water radiolysis. Moreover, no temperature dependence of this phenomenon has been characterized. To confirm the influence of β$^-$ radioactivity on the magnetic susceptibility measurements by the Evans' method, measurements have been carried out at various tritium (^3H_2O) concentrations in solution. The NMR spectrum is recorded on tert-butanol molecules diluted in the working and reference solution. To obtain a comfortable chemical shift difference $\Delta\delta$ on the NMR spectrum, analyses were performed with a fixed Nd(III) concentration in the temperature range 5-50°C.

The plot of the magnetic susceptibility versus the β$^-$ radioactivity in solution confirms a linear variation (**Figure 2**). The y-intercept (6.57.10^{-8}) provides a magnetic susceptibility value very close to the neodymium (III) magnetic susceptibility without β$^-$ emissions (**sample 6-9**, $\chi_M = 6.55\ (\pm 0.08)\cdot 10^{-8}$ m^3.mol^{-1}). The magnetic susceptibility of this cation is in good agreement with the theoretical value calculated for the free ion Nd^{3+} from the Curie law of Eq. **(10)** ($6.84\cdot 10^{-8}$ m^3.mol^{-1} at 298K), but also with magnetic susceptibility measurements performed on various Nd(III) compounds[30-35] which are between $5.99\cdot 10^{-8}$ m^3.mol^{-1} and $7.77\cdot 10^{-8}$ m^3.mol^{-1}. From this slope, we deduce that β$^-$ radioactivity contributes to an increase in magnetic susceptibility of **$6.09\cdot 10^{-25}$ m^6.mol^{-1}.Bq^{-1}** at 298K. This value is substantially lower than that obtained ($2.9\cdot 10^{-23}$ m^6.mol^{-1}.Bq^{-1}) in totally different conditions by ^{239}Np production, not confirming the assumption of a β$^-$ emissions influence on the ^{243}Am magnetic susceptibility variation over time[4]. Indeed, individual study of both radioactivity (α and β$^-$) shows that the formation and accumulation of secondary products by α water radiolysis is mainly responsible for this variation. It appears that for a given radioactivity of 400 GBq.L^{-1}, the β$^-$ emissions influence is twenty times less efficient ($2.44\cdot 10^{-10}$ m^3.mol^{-1}) than the α particles effect (≈ $4{,}49\cdot 10^{-9}$ m^3.mol^{-1}).

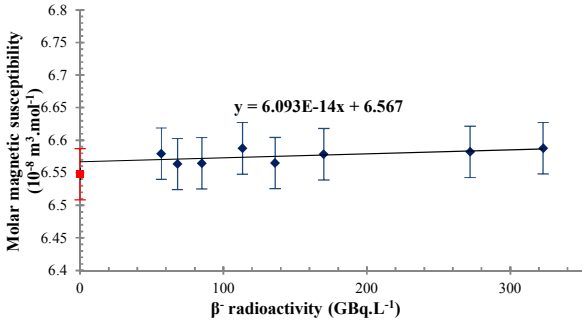

Figure 2: Molar magnetic susceptibility variation vs. β$^-$ radioactivity for Nd(III) samples in 1M perchloric medium at 298K.

The increase in magnetic susceptibility due to β$^-$-decay is found independent of temperature in the 5-50°C range and therefore does not follow a Curie law unlike the radicals formed by α radiolysis. The formation of radical species yields by β$^-$ water radiolysis is of the same order of magnitude as those determined for α radiolysis[36-38]. Nevertheless, the deposited energy by a β$^-$ particle (average energy 5.6 keV for ^{3}H) is extremely low compared to the deposited energy by an α particle (average energy 4.9 MeV for ^{233}U). It appears that the amount of radicals produced in solution is negligible and does not lead to the appearance of temperature dependence due to the presence of these radicals. Moreover, this kind of radiation led to an energy deposition on short trajectories (short tracks) promoting reactions between radicals in traces[39]. From this point of view, the lack of change in the Curie constant with the amount of tritiated water in solution is consistent with the radiolysis data revealing a small amount of radicals generated in solution and rapidly recombined in secondary species. The magnetic susceptibility variation revealed by these measures may be solely attributed to β$^-$ particles (electrons) produced by decay of ^{3}H isotope. This Temperature-Independent Paramagnetism (TIP) can be explained by the fact that the β$^-$ particles have meandering paths and which because of their speed does not diffuse as other species normally moving in a Brownian motion[40]. The thermal agitation of the medium having no impact on the direction of the electronic magnetic

moments in the NMR magnetic field B_0, β^- particles have a TIP behavior.

3.3. An(III) magnetic susceptibility measurements

The magnetic behavior of Pu(III), Am(III)[4] (**Figure 3**) and Cm(III) (**Figure ESI 7** of SI) was studied in 1M $HClO_4$ over the temperature range 273-328K.

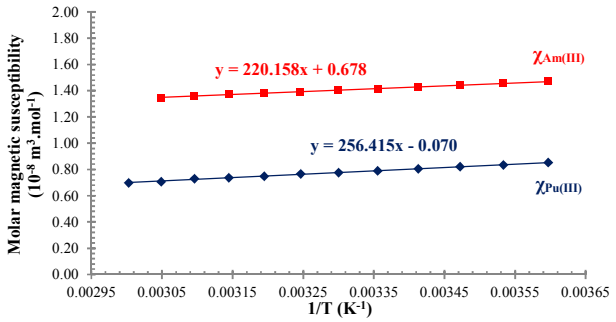

Figure 3: Magnetic susceptibility variation vs. 1/T for Am(III) (sample 1-1) and Pu(III) (sample 2) in 1M perchloric medium.

It appears that the magnetic susceptibilities of the trivalent cations Pu and Am, measured at 298K by the Evans' method ($\chi_{M,\,Pu(III)}$ = 0.79 (±0.02)·10^{-8} $m^3.mol^{-1}$; $\chi_{M,\,Am(III)}$ = 1.41 (±0.04)·10^{-8} $m^3.mol^{-1}$) are greater than the theoretical values calculated with the Curie law (Eq. **(10)**) ($\chi_{M,\,Pu(III)}$ = 0.39·10^{-8} $m^3.mol^{-1}$; $\chi_{M,\,Am(III)}$ = 0 $m^3.mol^{-1}$). An explanation involving the radicals effect formed by water radiolysis was proposed and demonstrated[4] as the cause of the magnetic susceptibility increase measured by the Evans' method. A magnetic susceptibility of 1.06·10^{-8} $m^3.mol^{-1}$ for Am(III) was determined but still remained higher than the value determined by Howland and Calvin[41] (χ_M = 0.47·10^{-8} $m^3.mol^{-1}$).

For Cm(III), the results obtained in this study ($\chi_{M,\,Cm(III)}$ = 31.9 (±0.8)·10^{-8} $m^3.mol^{-1}$ at 298K) are in good agreement with the Curie law (Eq. **(10)**) calculated from Hund's rules ($\chi_{M,\,Cm(III)}$ = 33.3·10^{-8} $m^3.mol^{-1}$ at 298 K). However, this new magnetic susceptibility value is different (≈ 10%) from a previous study performed in perchloric solution[1]. This gap can be connected to spectrometric techniques used to measure the concentration in radioactive elements. Indeed, the α spectrometry requires very high dilutions which can lead to increased measurement uncertainty and impacts the magnetic susceptibility values determined by this method (Eq. **(1)**). Then, the impurities in the working solution can also cause such deviations. Indeed, ^{244}Cm is a radioactive element with a short period ($T_{1/2}$ = 18.1 years) and it quickly generates a significant amount of ^{240}Pu which can lead to an overestimation of the magnetic susceptibility of this element. In our case, to remove plutonium formed by decay, extraction with TBP was previously performed on the mother solution of curium.

Considering the α and β^- emissions influence determined in this study, the magnetic behavior of stable An(III) (neither α nor β^- emission) with An = Pu, Am and Cm can be deducted by the following equation:

$$\chi_{M,corrected-\alpha,\beta^-} = \chi_M - \chi_{M,\alpha} - \chi_{M,\beta^-} \qquad \textbf{(17)}$$

Table 5 : α and β^- radioactivity in GBq.L^{-1}, measured and corrected molar magnetic susceptibility at 298K (10^{-8} $m^3.mol^{-1}$) and Curie constant (10^{-8} $m^3.K.mol^{-1}$) of the actinide samples.

Sample		α radioactivity	β^- radioactivity	χ_M	Slope *a*	$\chi_{M,\,corr.\,\alpha,\beta}$	Curie constant
Pu(III)	2	123	920	0.79 (±0.02)	256 (±6)	0.47 (±0.01)	176 (±6)
Am(III)	1-1	2940	/	1.41 (±0.04)	220 (±5)	0.65 (±0.01)	-7 (±5)
Cm(III)	5	862	/	31.9 (±0.8)	9432 (±236)	31.3 (±0.8)	9259 (±236)

After the radioactive correction, the magnetic susceptibility of Am(III) is independent of temperature in agreement with a TIP behavior (**Figure 4**). This is consistent with assumption made previously considering that alpha effect is only responsible for temperature dependence. Considering the isotopic composition of our samples and the radioactive decay influence (α and β^-) on measurements by the Evans' method, we deduce that the magnetic susceptibilities of Am(III) and Pu(III) are 0.65 (± 0.01)·10^{-8} $m^3.mol^{-1}$ and 0.47 (± 0.01)·10^{-8} $m^3.mol^{-1}$ respectively at 298K. The magnetic behavior with temperature of these two elements after subtracting α and β^- influences are shown **Figure 4**.

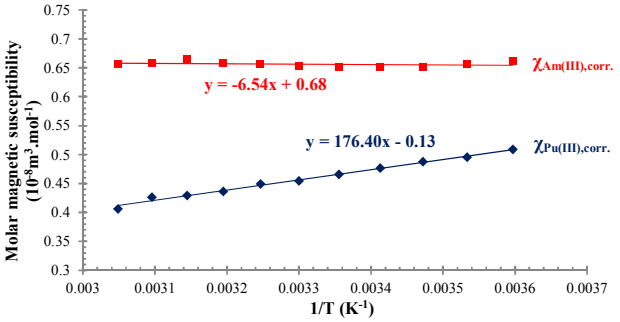

Figure 4: Corrected magnetic susceptibility variation vs. 1/T for Am(III) and Pu(III) cations in 1M perchloric medium.

Considering the isotopic composition of the Cm sample, we deduce that the magnetic susceptibility is 31.3 (± 0.8)·10^{-8} $m^3.mol^{-1}$ at 298K. This value and the temperature dependence of the magnetic susceptibility, shown in **Figure ESI 7** of SI, are not very different from the uncorrected value because of the high magnetic behavior of this element.

Regarding the Pu(III) cation, this value is slightly larger than that calculated with the Curie law and Hund's rules (0.39·10^{-8} $m^3.mol^{-1}$) but in agreement with the value measured by Howland and Calvin[41] in 1950 (χ_M = 0.47·10^{-8} $m^3.mol^{-1}$). These authors measured the magnetic susceptibility of this element by a bifilar suspension method with a concentration of 0.06M in radioactive element which is twice lower than the Pu(III) concentration used for our analysis. This lower concentration can lead to a decrease in the alpha effect part and thus a value closer to the actual Pu(III) magnetic susceptibility. However, the isotopic composition of the sample is not mentioned and no correction linked to the radicals formed by radiolysis can be applied.

This journal is © The Royal Society of Chemistry 2012

For Am(III), the experimental molar magnetic susceptibility is lower than the value measured by Howland and Calvin[41] ($\chi_M = 0.91 \cdot 10^{-8}$ $m^3.mol^{-1}$). However, this value does not take into account the alpha emissions effect on their magnetic susceptibility measurements. If we apply the same equation (Eq. **(17)**) to correct the magnetic susceptibility value obtained by these authors, we deduce that the magnetic susceptibility of Am(III) is $0.65 \cdot 10^{-8}$ $m^3.mol^{-1}$. A perfect agreement is observed with our value despite the different methods used.

Recently Apostolidis *et al.* have studied the magnetic properties of crystalline aquo compounds $[An(H_2O)_9](CF_3SO)_3$ (An = U – Am) which are ideal probes for these ions in aqueous phase[3]. They measured a magnetic susceptibility on solid compound Pu(III) aquo ion of $0.34 \cdot 10^{-8}$ $m^3.mol^{-1}$ at 298K. For Am(III), they indicate that the magnetic susceptibility is consistent with a non-magnetic behavior (TIP) without mentioning the value which is lower than that of Pu(III). These results are in contradiction with our experimental results since the magnetic susceptibility is clearly larger for Am(III) than for Pu(III) for the whole range of temperatures (see **Figure 4**). However, the variation of the magnetic susceptibility with temperature of Pu(III) in solution is three times larger than the one for the solid compound $[Pu(H_2O)_9](CF_3SO)_3$ measured by Apostolidis *et al.*[3]. This difference between solution and solid phase measurements may be responsible for the difference in the ordering of the magnetic susceptibilities of Pu(III) and Am(III) at room temperature.

Finally, the Cm(III) magnetic susceptibility appears in the range of published values and obtained in the solid Cm_2O_3 compounds (29.64 – $32.89 \cdot 10^{-8}$ $m^3.mol^{-1}$)[42, 43].

3.4. Theoretical calculations

Electronic states and magnetic susceptibility. Energy gaps calculated with SO-CASPT2 for Pu(III), Am(III) and Cm(III) aquo complexes are provided **Table 6**. For Pu(III) and Cm(III) which have an odd number of electrons, all states are doubly degenerate Kramers doublets (KD) and g factors are calculated for each doublet.

Table 6: Energy gaps ΔE_I (cm^{-1}) and g factors calculated with SO-CASPT2, free ion levels in zero field for $[Pu(H_2O)_9]^{3+}$, $[Am(H_2O)_9]^{3+}$ and $[Cm(H_2O)_9]^{3+}$. All states for $[Pu(H_2O)_9]^{3+}$ and $[Cm(H_2O)_9]^{3+}$ are KDs.

	Free ion level	ΔE_I	g factors		
			g_1	g_2	g_3
$[Pu(H_2O)_9]^{3+}$	$^6H_{5/2}$	0	0.68	0.56	0.53
		139	1.01	0.16	0.12
		230	1.35	0.47	0.11
$[Am(H_2O)_9]^{3+}$	$^7F_0$	0		/	
	$^7F_1$	2309		/	
		2314		/	
		2430		/	
$[Cm(H_2O)_9]^{3+}$	$^8S_{7/2}$	0	11.9	2.7	1.9
		11	9.3	5.5	1.7
		18	7.3	6.0	0.5
		31	8.9	4.3	1.7

$[Pu(H_2O)_9]^{3+}$:

For the Pu^{3+} cation, the crystal field of the water molecules splits the free ion ground level $^6H_{5/2}$ in three KDs at 0, 139 and 230 cm^{-1} respectively. According to the values of the g factors, these states are weakly anisotropic and do not have large magnetic moments in accordance with the value of $2g_JJ$=1.43. The magnetic field splits the KDs in two states. Due to the large zero-field splitting of the ground level, the condition $E_I \ll kT$ is not fulfilled at 298 K and the Curie law limit of Eq. **(7)** is not reached. Each state I contributes to the magnetization by its magnetic moment $\boldsymbol{M}_I(\boldsymbol{B})$ and its Bolzmann weight $P_I = e^{-(E_I(\boldsymbol{B})-E_0(\boldsymbol{B}))/kT}$. The magnetization results from the contribution of the successive levels and may be described as a truncated sum in Eq. **(5)** by the following equation:

$$M_{\boldsymbol{u}}^{\boldsymbol{0\to k}} = \frac{\sum_{I=0}^{K} \boldsymbol{M}_I(\boldsymbol{B})\, P_I}{\sum_{I=0}^{K} P_I}$$

The contributions of each state to the Pu(III) magnetization and magnetic susceptibility are summarized in **Table 7**.

Since the energy gap between the ground and the first excited KD is larger than kT ≈ 200 cm^{-1}, the magnetic behavior of Pu^{3+} at room temperature is dominated by the first KD since the two other KDs are only partially populated. For comparison, in the case of a small zero-field splitting, the Curie law limit would give M=0.0076 μ_B in all directions at 298 K and B=9.4 T. The first excited level of the free ion, the level $^6H_{7/2}$, lies 2600 cm^{-1} above the ground level; this manifold is not thermally populated. But, those states may interact with the J=5/2 manifold by second-order Zeeman interaction. Results of **Table 7** are obtained by the diagonalization of Hamiltonian of Eq. **(3)** within the basis of the first 40 electronic states and therefore take into account the Zeeman coupling with highly excited states. In order to analyse the effect of the states arising from larger values of J, the same calculations have been performed but restricting the diagonalization to the 6 first states. Results are given in **Table ESI 3** of the SI. The magnetic susceptibility is much smaller in this case indicating that, the excited states play a quantitative role on the magnetic behaviour by second order Zeeman interaction. The importance of second order effects is due to the relatively small first order Zeeman interaction in the ground J manifold (small g_JJ).

To conclude, the magnetic susceptibility of the aquo Pu(III) cannot be described by the Curie law : i) the splitting of the ground J manifold by crystal field is too large to neglect the zero-field splitting ii) Zeeman interaction with the excited J levels plays a quantitative role.

$[Am(H_2O)_9]^{3+}$:

The ground level of Am(III) is $^7F_0$: it is a non-degenerate and non-magnetic state. States arising from the first excited level $^7F_1$ lie above 2300 cm^{-1} (see **Table 6**) and are not populated at room temperature. The magnetic behavior arises from second-order Zeeman effect according to Eq. **(12)**: it is TIP. Under the magnetic field, a very small change in the energy of different states can be observed. Contributions of each state I to the magnetic susceptibility of Am(III) aquo complex are given in **Table ESI 7** of SI. These results are obtained by the diagonalization of Hamiltonian of Eq. **(3)** within 40 electronic states but results are the same when this diagonalization is limited to four states, namely the states arising from $^7F_0$ and $^7F_1$. It shows that the states arising from higher J levels do not contribute by second order Zeeman interaction. It should be outlined that the susceptibility of the TIP Am(III) whose ground state is non-magnetic at first order is larger than the one

of Pu(III) aquo complex whose ground manifold is magnetic at first order.

Table 7: Energy gaps ΔE_I (cm^{-1}), magnetic moments M_I^u in direction u (μ_B), Boltzmann weights P_I, truncated magnetizations $M_u^{0\to k}$ (μ_B) and magnetic susceptibility χ_M ($m^3.mol^{-1}$) for $[Pu(H_2O)_9]^{3+}$ in a magnetic field of 9.4 Tesla and at T=298 K. Diagonalization of Hamiltonian of Eq. (3) is performed with 40 electronic states. x, y and z are the principal directions of the tensor g of the ground KD.

	ΔE_I	M_I^μ	P_I	$M_u^{0\to k}$	χ_M
Direction z	0	0.351	1.00	0.350	
	3.0	-0.329	0.99	0.012	$0.98\cdot10^{-8}$
	138	0.440	0.51	0.107	
	142	-0.431	0.50	0.011	$0.85\cdot10^{-8}$
	229	0.454	0.33	0.060	
	233	-0.456	0.32	0.009	$\mathbf{0.75\cdot10^{-8}}$
Direction x	0	0.280	1.00	0.280	
	2.3	-0.246	0.99	0.019	$1.39\cdot10^{-8}$
	139	0.099	0.51	0.035	
	140	-0.089	0.51	0.014	$1.05\cdot10^{-8}$
	230	0.135	0.33	0.026	
	231	-0.152	0.33	0.010	$\mathbf{0.75\cdot10^{-8}}$
Direction y	0	0.292	1.00	0.292	
	2.4	-0.266	0.99	0.015	$1.10\cdot10^{-8}$
	139	0.262	0.51	0.065	
	141	-0.255	0.51	0.011	$0.85\cdot10^{-8}$
	229	0.533	0.33	0.063	
	234	-0.538	0.32	0.010	$\mathbf{0.74\cdot10^{-8}}$

$[Cm(H_2O)_9]^{3+}$:

The ground level of Cm(III) is the $^8S_{7/2}$ level ; this state is a pure spin state and is not split by first-order spin-orbit coupling. In the Cm(III) aquo complex, this state split in four KDs due to second-order spin-orbit coupling with the states arising from the excited levels which lie above 21300 cm^{-1}. Therefore, the zero-field splitting of the ground J=7/2 manifold is smaller than 200 cm^{-1} (see **Table 6**). The contributions of each state to magnetic susceptibility are given in **Table ESI 9** of SI. In this case, $E_I \ll kT$, and at room temperature, all states are largely populated and we are close to the Curie law limit. Since $2g_JJ$=14 is large, the Cm(III) aquo complex has a much larger suceptibility than the two previous ones.

Ligand field effect: The magnetic susceptibility depends linearly on 1/T in the 250-350 K range, in accordance with Eq. **(14)**. *C* and χ_{TI} are summarized for aquo complexes of Pu(III), Am(III) and Cm(III) in Error! Reference source not found..

Table 8: Curie constants C (10^{-8} $m^3.K.mol^{-1}$) and temperature-independent susceptibilities χ_{TI} (10^{-8} $m^3.mol^{-1}$) from Hund's rules, SO-CASPT2 and experiment for $[Pu(H_2O)_9]^{3+}$, $[Am(H_2O)_9]^{3+}$ and $[Cm(H_2O)_9]^{3+}$ complexes.

	C Hund	C SO-CASPT2	χ_{TI} SO-CASPT2	C exp	χ_{TI} exp
$[Pu(H_2O)_9]^{3+}$	113	111	0.37	176 (±6)	-0.13 (±0.01)
$[Am(H_2O)_9]^{3+}$	0	-0.2	0.86	-7 (±5)	0.68 (±0.02)
$[Cm(H_2O)_9]^{3+}$	9902	9233	0.12	9259 (±236)	0.30 (±0.01)

$[Pu(H_2O)_9]^{3+}$:

The comparison between experimental and calculated data shows differences: the experimental slope is much larger and the temperature independent parts have opposite signs (**Figure ESI 8** of SI). The experimental χ_{TI} is diamagnetic and does not correspond to the mechanism of Eq. **(14)** where χ_{TI} is necessarily positive. So far, we neglected diamagnetic contribution but in this particular case of low magnetic susceptibility value, it should be taken into account. This behavior seems to characterize an experimental value of χ_{TI} close to 0. This difference can be also attributed to experimental error on extrapolation at the origin of magnetic susceptibility curves versus 1/T because of the short temperature range.

In order to better analyze the parameters determining this susceptibility, SO-CASPT2 calculations on the free ion Pu(III) have been performed (**Table ESI 2**). The calculation restricted to $^6H_{5/2}$ level leads to a Curie law with a C close to $113\cdot10^{-8}$ $m^3.K.mol^{-1}$ as expected in a pure LS scheme. Taking into account the next level $^6H_{7/2}$ slightly changes the value of C and gives rise to an important χ_{TI} due to the low lying $^6H_{7/2}$ (1762cm^{-1}). Increasing the number of levels involved in the spin-orbit coupling calculations shows that the ^4G term plays a key role. This term is the fourth spin quartet and lies 14500 cm^{-1} above the ground term according to our calculations. The coupling between the ^6H and ^4G terms increases the gap with between the $J = 5/2$ and $J = 7/2$ levels, increases the Curie constant and decreases χ_{TI}. For the free ions, SO-CASSCF results, which do not consider dynamical correlation, may be compared to the more accurate results obtained with the GRASP code (**Table ESI 1**): it shows that SO-CASSCF energies are overestimated by about 10 %.

Different solvation environments have been considered, varying either the metal-water distance or the number of water molecules: results are summarized in **Table ESI 4**. The results do not depend strongly on the description of the solvent; χ_{TI} is almost independent on the solvation sphere and close to the value of the free ion. The Curie constant decreases with the metal-ligand distance from $144\cdot10^{-8}$ $m^3.K.mol^{-1}$ in the free ion to $80\cdot10^{-8}$ $m^3.K.mol^{-1}$ in $[Pu(H_2O)_8]^{3+}$ with a short distance. The susceptibility at 298 K is about $0.75\cdot10^{-8}$ $m^3.K.mol^{-1}$, a value close to the uncorrected experimental value. To conclude, the calculation show that the susceptibility of Pu(III) have a large temperature-independent paramagnetic contribution due to the coupling with the first excited $J = 7/2$ level and that the LS scheme is not sufficient to describe quantitatively the magnetic properties of this ion: spin-orbit coupling with an excited spin quartet plays a quantitative role. The discrepancy between experiment and calculations arises mainly from temperature-independent part: this contribution is shown to be negative by the experiment and is not reproduced in the present calculations.

$[Am(H_2O)_9]^{3+}$:

As for Pu(III), we performed the calculations on the free ion: results are given in **Table ESI 6** of the SI. Since the ground state is a J=0 level, susceptibility arises only by second order Zeeman coupling with the J=1 level. Higher levels do not contribute to the Van Vleck equation (Eq. **(9)**). In the case of TIP (Eq. **(12)**), the magnetic susceptibility is determined by the energy gap with the J=1 level. As shown in **Table ESI 6**, there are three LS states contributing to this gap ^7F, ^5D and ^3P. It is noteworthy that the triplet state plays such a fundamental role while it does not couple directly with the septet

This journal is © The Royal Society of Chemistry 2012

ground state. The value of χ_{TI} obtained with these three states and the Van Vleck equation reduced to J=0 and J=1 levels is describes correctly the experimental value (**Figure ESI 6** of SI). The comparison between SO-CASSCF and GRASP (**Table ESI 5**) shows that like for Pu^{3+}, SO-CASSCF tends to overestimate the energy gaps. The effect of correlation is important, since the gap between the J=0 and J=1 levels increases from 2010 to 2570 cm^{-1}.

The effect of the ligands is an increase of the value of χ_{TI} due to a smaller gap with the states arising from the J=1 level. The effect of the coordination sphere has been analyzed with an elongated and contracted Am-OH_2 distance. Results are summarized **Table 9**: the size of the coordination sphere plays a role for Am(III) contrarily to Pu(III) by affecting the J=1 energy gap. This energy gap has been determined by optical spectroscopy in several matrices ($LaCl_3$ and ThO_2). For Am^{3+} ions diluted in $LaCl_3$[44-46], the gap is about 2750 cm^{-1} while diluted in ThO_2[47] it is 2637 cm^{-1}. These values are larger than those calculated by SO-CASPT2 for the aquo complex : since this gap is underestimated, the value of the susceptibility is too large. This error in the calculation of the gap may due to the calculation of the correlation.

Table 9: Energy gaps ΔE_I in cm^{-1}, Boltzmann weights P_I and magnetic susceptibility χ_M in $m^3.mol^{-1}$ for $[Am(H_2O)_9]^{3+}$, $[Am(H_2O)_9]^{3+}$+0.1Å and $[Am(H_2O)_9]^{3+}$-0.1Å in a magnetic field of 9.4 Tesla and at T=298 K. Diagonalization of Hamiltonian of Eq. (1) is performed with 4 electronic states.

	Free ion electronic states	ΔE_I (cm^{-1})	P_I	χ_M ($m^3.mol^{-1}$)
$[Am(H_2O)_9]^{3+}$ + 0,1Å	$^7F_0$	0	1	$0.815 \cdot 10^{-8}$
	$^7F_1$	2369	0.00001	
		2377	0.00001	
		2567	0	
$[Am(H_2O)_9]^{3+}$	$^7F_0$	0	1	$0.865 \cdot 10^{-8}$
	$^7F_1$	2309	0.00002	
		2314	0.00002	
		2430	0.00001	
$[Am(H_2O)_9]^{3+}$ - 0,1Å	$^7F_0$	0	1	$0.930 \cdot 10^{-8}$
	$^7F_1$	2165	0.00003	
		2226	0.00002	
		2317	0.00001	

To conclude, the magnetic susceptibility of Am(III) aquo complex is close to the one of the free ion : it is determined by second-order Zeeman coupling with the J=1 excited manifold and the gap with this states implies a spin-orbit coupling between the three LS states ^7F, ^5D and ^3P. The effect of the coordination sphere is a decrease of this gap and consequently an increase of the value of χ_{TI}.

$[Cm(H_2O)_9]^{3+}$:

The SO-CASPT2 magnetic susceptibility of $[Cm(H_2O)_9]^{3+}$ is in good agreement with the experimentally one. It is explained by the fact that it is a pure spin magnetism and that the first excited level lies high in energy and does not impact the magnetic susceptibility. The comparison between SO-CASSCF and GRASP (**Table ESI 8**) shows that as for Pu^{3+} and Am^{3+}, the energy gaps are overestimated by about 10 %. The dynamical correlation (comparison between SO-CASSCF and SO-CASPT2) reduces the gap between the ground J=5/2 and J=7/2 levels by about 5000 cm^{-1}. And finally, the effect of the ligands decreases this gap to 21300 cm^{-1}. Experimental measurements made on the aquo ion[48] and diluted in a $LaCl_3$ matrix[49] reveals an isolated electronic level at 17000 cm^{-1}. This value is lower than the calculated one by 4300 cm^{-1}: it shows that SO-CASPT2 is not quantitative to reproduce the full energetic spectrum of aquo Cm^{3+} . However, this difference doesn't affect the Cm^{3+} magnetic susceptibility because this high electronic state is not involved in the magnetic properties. The free ion and aquo Cm^{3+} magnetizations (**Table ESI 9** and **Table ESI 10** respectively) reveal very similar behaviors. In this case, the crystal field is masked by the magnetism magnitude and low energy electronic states structure has a negligible influence on the calculation.

4. Conclusion

The study made by the Evans method on ^{233}U have confirmed the observations performed previously with ^{241}Am which is to say that the presence of α emissions contributes to the increase of the magnetic susceptibility[4]. From a radioactivity of 30 $GBq.L^{-1}$, the Curie constant increases which can be ascribed to a radical concentration increase in solution. Beyond this radioactivity, saturation of radiolytic interaction induced by a rapid recombination of radicals formed by water radiolysis tends to stabilize this progress. The whole phenomenon can be modeled by a logarithmic function to establish a relationship between α radioactivity in solution and the magnetic susceptibility measured by the Evans' method. Similarly, measurements made on tritiated water (^3H_2O), confirm the previous observations on ^{243}Am showing that β^- emissions increase the magnetic susceptibility measurements made by the Evans' method. However, this increase is twenty times lower than that generated by α emission for the same radioactivity (400 $GBq.L^{-1}$) unlike the previous results on ^{239}Np predicting a higher influence of these particles. This mistake can be explained by the formation and significant accumulation of degradation products by α water radiolysis. Moreover, unlike α emission, it has been noticed that the electrons generated in solution induce a temperature independent magnetic phenomenon.

The magnetic susceptibilities of Pu(III) and Am(III) ions in 1M perchloric medium, once corrected by the effect of their radioactive decay (α and β^- emissions), are $0.466 \cdot 10^{-8}$ $m^3.mol^{-1}$ and $0.650 \cdot 10^{-8}$ $m^3.mol^{-1}$ respectively at 298K. The calculations made by SO-CASPT2 overestimate these values. The difficulties of the theoretical description arise from the large number of LS states participating to the ground free ion level, to the large effect of the dynamical correlation in actinide complexes and to the important effect of the solvent: for these two ions, the first excited level plays a crucial role and determines the temperature independent part of the susceptibility. From an experimental point of view, TIP values determined by Evan's method lack accuracy due to the short temperature ranges too. Despite these problems raised for these cations of low paramagnetic susceptibilities, calculations and experiments confirm some trends, namely the change in Pu(III) and Am(III) magnetic susceptibilities ordering for a temperature of about -53°C (±8°C).

Regarding the Cm(III), a good description of magnetic behavior is obtained for the aquo complex for which the coupling with high-energy electronic states does not impact the magnetic properties.

To conclude, these calculations cannot be considered predictive of accurate magnetic susceptibility values in solution although the

magnitude is respected but rather as a necessary tool for the understanding of the magnetic properties of these cations.

Acknowledgements

The authors acknowledge Dr. J-C. Broudic for his helpful contribution to the development of tritium experiments and Dr. D. Guillaumont for geometry optimizations of aquo ions.

References

1. T. F. Wall, S. Jan, M. Autillo, K. L. Nash, L. Guerin, C. L. Naour *et al.*, *Inorg. Chem.*, 2014**, 53**, 2450-2459.
2. D. F. Evans, *J. Chem. Soc.*, 1959, 2003-2005.
3. C. Apostolidis, B. Schimmelpfennig, N. Magnani, P. Lindqvist-Reis, O. Walter, R. Sykora *et al.*, *Angew. Chem., Int. Ed.*, 2010**, 49**, 6343-6347.
4. M. Autillo, P. Kaden, A. Geist, L. Guerin, P. Moisy, C. Berthon, *Phys. Chem. Chem. Phys.*, 2014**, 16**, 8608-8614.
5. C. Ferradini, J. P. Jay-Gerin, *Can. J. Chem.*, 1999**, 77**, 1542-1575.
6. G. V. Buxton, J. F. Wishart, M. Mostafavi, I. Lampre, G. Baldacchino, B. Hickel, Part I : Primary radiation-induced phenomena. In *Radiation chemistry*, EDP Sciences ed.; M. Spotheim-Maurizot, M. Mostafavi, T. Douki, J. Belloni Eds.; 2008, 3-64.
7. J. T. Coutinho, M. A. Antunes, L. C. J. Pereira, H. Bolvin, J. Marcalo, M. Mazzanti *et al.*, *Dalton Trans.*, 2012**, 41**, 13568-13571.
8. M. A. Antunes, I. C. Santos, H. Bolvin, L. C. J. Pereira, M. Mazzanti, J. Marcalo *et al.*, *Dalton Trans.*, 2013**, 42**, 8861-8867.
9. R. A. Penneman, T. K. Keenan, *The radiochemistry of americium and curium*. U. S. Atomic Energy Commission: Los Alamos, 1960.
10. D. Cohen, *J. Inorg. Nucl. Chem.*, 1961**, 18**, 211-218.
11. F. Aquilante, L. De Vico, N. Ferre, G. Ghigo, P.-A. Malmqvist, P. Neogrady *et al.*, *J. Comput. Chem.*, 2010**, 31**, 224-247.
12. P. G. Allen, J. J. Bucher, D. K. Shuh, N. M. Edelstein, I. Craig, *Inorg. Chem.*, 2000**, 39**, 595-601.
13. S. Skanthakumar, M. R. Antonio, R. E. Wilson, L. Soderholm, *Inorg. Chem.*, 2007**, 46**, 3485-3491.
14. T. Stumpf, C. Hennig, A. Bauer, M. A. Denecke, T. Fanghanel, *Radiochim. acta*, 2004**, 92**, 133-138.
15. B. Brendebach, N. L. Banik, C. M. Marquardt, J. Rothe, M. A. Denecke, H. Geckeis, *Radiochim. acta*, 2009**, 97**, 701-708.
16. P. D'Angelo, F. Martelli, R. Spezia, A. Filipponi, M. A. Denecke, *Inorg. Chem.*, 2013**, 52**, 10318-10324.
17. P. G. Allen, J. J. Bucher, D. K. Shuh, N. M. Edelstein, T. Reich, *Inorg. Chem.*, 1997**, 36**, 4676-4683.
18. M. J. Frisch, G. W. Trucks, H. B. Schlegel, G. E. Scuseria, M. A. Robb, J. R. Cheeseman *et al. Gaussian 09*, Gaussian, Inc.: Wallingford, CT, USA, 2009.
19. X. Cao, M. Dolg, H. Stoll, *J. Chem. Phys.*, 2003**, 118**, 487-496.
20. B. O. Roos, R. Lindh, P.-A. Malmqvist, V. Veryazov, P.-O. Widmark, A. C. Borin, *J. Phys. Chem. A*, 2008**, 112**, 11431-11435.
21. B. O. Roos, R. Lindh, P. A. Malmqvist, V. Veryazov, P. O. Widmark, *J. Phys. Chem. A*, 2004**, 108**, 2851-2858.
22. B. O. Roos, P. R. Taylor, P. E. M. Siegbahn, *Chem. Phys.*, 1980**, 48**, 157-173.
23. K. Andersson, P. A. Malmqvist, B. O. Roos, A. J. Sadlej, K. Wolinski, *J. Phys. Chem.*, 1990**, 94**, 5483-5488.
24. P. A. Malmqvist, B. O. Roos, B. Schimmelpfennig, *Chem. Phys. Lett.*, 2002**, 357**, 230-240.
25. B. A. Hess, C. M. Marian, U. Wahlgren, O. Gropen, *Chem. Phys. Lett.*, 1996**, 251**, 365-371.
26. H. Bolvin, *Chemphyschem*, 2006**, 7**, 1575-1589.
27. K. G. Dyall, I. P. Grant, C. T. Johnson, F. A. Parpia, E. P. Plummer, *Comput. Phys. Commun.*, 1989**, 55**, 425-456.
28. J. E. Fanning, C. N. Trumbore, P. G. Barkley, J. H. Olson, *J. Phys. Chem.*, 1977**, 81**, 1264-1268.
29. J. C. Muller, C. Ferradini, J. Pucheault, *Int. J. Radiat. Phys. Chem.*, 1975**, 7**, 635-641.
30. R. Baggio, R. Calvo, M. T. Garland, O. Pena, M. Perec, A. Rizzi, *Inorg. Chem.*, 2005**, 44**, 8979-8987.
31. L. Beaury, J. Derouet, P. Porcher, *J. Alloys Compd.*, 1995**, 225**, 28-34.
32. K. N. Chattopadhyay, D. Neogy, D. Bisui, P. Paul, P. K. Chakrabarti, *J. Phys. Chem. Solids*, 1999**, 60**, 709-713.
33. H. Hacker, M. S. Lin, *Solid State Commun.*, 1968**, 6**, 379-&.
34. S. T. Hatscher, W. Urland, *Mater. Res. Bull.*, 2003**, 38**, 99-112.
35. J. M. Lock, *Proc. Phys. Soc., London, Sect. B*, 1957**, 70**, 566-576.
36. E. Collinson, F. S. Dainton, J. Kroh, *Proc. R. Soc. London, Ser. A*, 1962**, 265**, 430-&.
37. E. Collinson, J. Kroh, F. S. Dainton, *Proc. R. Soc. London, Ser. A*, 1962**, 265**, 422-&.
38. G. Lemaire, Pucheaul.J, Ferradin.C, *J. Phys. Chem.*, 1972**, 76**, 1542-&.
39. S. Mustaree, J. Meesungnoen, S. L. Butarbutar, P. Causey, C. R. Stuart, J.-P. Jay-Gerin, *Rsc Advances*, 2014**, 4**, 43572-43581.
40. G. R. Freeman, *Kinetics of Nonhomogeneous Processes: A Practical Introduction for Chemists, Biologists, Physicists, and Materials Scientists*. Wiley: 1987.
41. J. J. Howland, M. Calvin, *J. Chem. Phys.*, 1950**, 18**, 239-243.
42. L. R. Morss, J. Fuger, J. Goffart, R. G. Haire, *Inorg. Chem.*, 1983**, 22**, 1993-1996.
43. S. E. Nave, R. G. Haire, P. G. Huray, *Phys. Rev. B*, 1983**, 28**, 2317-2327.
44. W. T. Carnall, *J. Chem. Phys.*, 1992**, 96**, 8713-8726.
45. J. G. Conway, *J. Chem. Phys.*, 1964**, 40**, 2504-&.
46. W. T. Carnall, *J. Less-Common Met.*, 1989**, 156**, 221-235.
47. S. Hubert, P. Thouvenot, N. Edelstein, *Phys. Rev. B*, 1993**, 48**, 5751-5760.
48. W. T. Carnall, K. Rajnak, *J. Chem. Phys.*, 1975**, 63**, 3510-3514.
49. J. B. Gruber, W. R. Cochran, J. G. Conway, A. T. Nicol, *J. Chem. Phys.*, 1966**, 45**, 1423-1427.

 This journal is © The Royal Society of Chemistry 2012